Glassy polymers' strain-hardening moduli scale with their statistical-segment volumes

Robert S. Hoy*
Department of Physics, University of South Florida, Tampa, Florida 33620, USA

(Received 20 November 2025; accepted 26 March 2026; published 8 April 2026)

Using molecular dynamics simulations, we show that a widely accepted theoretical prediction for glassy-polymeric strain-hardening moduli ($G_R \propto \rho_e$, where ρ_e is the entanglement density) fails badly for semiflexible polymers. By postulating that the length, energy, and strain scales controlling G_R are the Kuhn length ℓ_K and statistical-segment length $b = \sqrt{\ell_0 \ell_K}$ (where ℓ_0 is the backbone bond length), the intermonomer binding energy u_0, and the incremental elastic strain $\mathcal{S}_c$ required to activate Kuhn-segment-scale plastic rearrangements, we develop a scaling theory predicting that $G_R = \mathcal{S}_c(u_0/\ell_0^3)(b/\ell_0)^3$ in the athermal limit. This prediction agrees quantitatively with the simulated G_R values for athermal uniaxial-stress extension, and semiquantitatively with the values for athermal constant-volume simple shear, for bead-spring polymer glasses spanning a range of ℓ_K/ℓ_0 that is wider than the range spanned by real systems.

DOI: 10.1103/6qn6-9zrz

I. INTRODUCTION

Understanding glassy-polymeric strain hardening has been a long-standing challenge. Early efforts [1] focused on the observation that the normal-stress difference at strains well beyond yield takes the form $\Delta\sigma(\bar{\lambda}) \simeq \sigma_{\text{flow}} + G_R g(\bar{\lambda})$, where σ_{flow} is the plastic flow stress, G_R is the strain-hardening modulus, and $g(\bar{\lambda})$ is a dimensionless function of the macroscopic stretch tensor $\bar{\lambda}$. Rubber-elasticity-based theories [2–4] assume that $g(\bar{\lambda}) = \partial\tilde{g}/\partial\bar{\lambda}$, where $\tilde{g}(\bar{\lambda})$ describes the deformation-induced reduction in the configurational entropy. These theories predict that $G_R = (\rho/N_e)k_BT \equiv \rho_e k_B T$ where ρ is the monomer number density, N_e is the entanglement length, $\rho_e \equiv \rho/N_e$ is the entanglement density, and T is temperature. They have many flaws that have been discussed at great length in the literature; in particular, they dramatically fail to predict both the magnitude and the temperature dependence of glassy-polymeric G_R [5–9].

Haward pointed out [5] that fitting stress-strain curves for various polymer glasses to $\Delta\sigma(\bar{\lambda}) \simeq \sigma_{\text{flow}} + \rho_e k_B T g(\bar{\lambda})$ produces estimates of ρ_e that are up to 2 orders of magnitude larger than estimates obtained from independent measurements of their parent melts' plateau moduli G_N^0 (i.e., $\rho_e \simeq \rho_e^{\text{melt}} \equiv 5G_N^0/4k_BT_{\text{melt}}$). Noting that the same functional forms $g(\bar{\lambda})$ dominate the large-strain response of hyperelastic (neo-Hookean) materials [5], and that the prefactors C obtained from plugging experimentally measured values of G_R into the equation $G_R = C\rho_e^{\text{melt}}k_BT$ are strongly chemistry dependent [6], he suggested that G_R is primarily determined by polymer glasses' local Kuhn-segment-scale structure rather than by entanglements. Since then, a great deal of experimental and theoretical work has supported the idea that strain hardening is closely related to plastic flow and hence to local inter- and intrasegmental interactions (see Refs. [10,11] for recent reviews).

The idea that strain hardening is only secondarily related to entanglement, however, remains controversial. Van Melick *et al.*'s careful study of polystyrene-polypropylene oxide (PS-PPO) blends and variably-crosslinked PS showed that systems' measured G_R were linearly proportional to ρ_e^{melt} [7]. Simulations of flexible polymer glasses also found that $G_R \sim \rho_e \simeq \rho_e^{\text{melt}}$ [12–15], and since there has (to date) been little to no experimental evidence to contradict this notion, it remains widely accepted. As a consequence, because a *simple* theory that quantitatively relates G_R to microscopic-structural parameters has remained elusive, it is tempting to assume that G_R depends on these parameters in the same way that G_N^0 does. For example, since the packing model [16,17] asserts that $G_N^0\ell_K^3/k_BT_{\text{melt}} \sim (\ell_K/p)^3$ [where $p = (\rho\ell_0\ell_K)^{-1}$ is the packing length] and correctly predicts the G_N^0 values for all flexible polymers [18], one could assume that these polymers' $G_R \sim G_N^0 \sim p^{-3} \sim (\rho\ell_0\ell_K)^3$. This hypothesis, however, has not been systematically investigated. Experimental tests are impeded by the chemistry-dependent C, and previous comprehensive simulations focusing on strain hardening (e.g., Refs. [13–15]) have examined only a narrow range of ℓ_K.

Moreover, recent studies have shown that $G_N^0 \sim p^{-3}$ scaling breaks down as ℓ_K/p increases into the semiflexible regime where $N_e \lesssim 4C_\infty$ (here C_∞ is the Flory characteristic ratio) [19–22]. The semiflexible conjugated polymers (SCPs) that populate this regime are currently attracting great interest owing to their unique combination of electronic and mechanical properties [22–27]. Recent molecular dynamics simulations have suggested [28,29] that these polymers can form ductile glasses, contrary to previous expectations [30]. However, their strain-hardening behavior has not yet been systematically investigated, raising the question of whether they obey the typical $G_R \sim G_N^0 \propto \rho_e$ trend.

In this paper, by reanalyzing simulation data from Ref. [29], we show that they do not. The linear $G_R \sim \rho_e$ scaling breaks down as ℓ_K/p increases into the semiflexible regime; in this regime, G_R is supralinear in ρ_e. On the other

*Contact author: rshoy@usf.edu

hand, we find that—at least for uniaxial-stress extension—$G_R \propto (\ell_K/\ell_0)^{3/2}$ to within our statistical uncertainties on G_R and ℓ_K, for both flexible and semiflexible polymer glasses. By assuming (i) that these glasses act like neo-Hookean solids [5,6], and (ii) that the range of their elastic intermonomer interactions is b, or equivalently that their plastic rearrangements mobilize a volume of order b^3, we formulate a simple scaling theory that predicts this 3/2 power law, and also the prefactor G_0 in the observed $G_R = G_0(\ell_K/\ell_0)^{3/2}$ relationship to within a factor of order one. In particular, we argue that

$$\begin{aligned}\Delta\sigma &= \sigma_{\rm flow} + \mathcal{S}_{\rm c}\big(u_0/\ell_0^3\big)(\ell_K/\ell_0)^{3/2} g(\bar{\lambda}) \\ &= \sigma_{\rm flow} + \mathcal{S}_{\rm c}\big(u_0/\ell_0^3\big)(b/\ell_0)^3 g(\bar{\lambda}) \end{aligned} \quad (1)$$

in the athermal limit, where $\mathcal{S}_{\rm c}$ is the incremental elastic strain required to activate these rearrangements.

II. MODEL AND METHODS

All simulations were performed using LAMMPS [31], and employed the semiflexible, breakable-bond variant of the Kremer-Grest model [32–34]. Monomers have mass m and interact via the truncated and shifted Lennard-Jones potential $U_{\rm LJ}(r) = 4u_0[(a/r)^{12} - (a/r)^6 - (a/r_c)^{12} + (a/r_c)^6]$, where u_0 is the intermonomer binding energy, a is the monomer diameter, and $r_c = 2^{7/6}a$ is the cutoff radius. This value of r_c, which is twice the distance at which Lennard-Jones forces vanish (i.e., $2^{1/6}a$), is a convenient choice for r_c that includes monomers within the first two coordination shells and has been used in several recent simulations of glassy-polymer mechanics [28,29,35]. Previous studies found that G_R increases linearly with $\sigma_{\rm flow}$ as r_c is varied over the range $1.5 \leqslant r_c/a \leqslant 2.6$ [13]. Covalent bonds are modeled using a standard quartic potential [34] $U_{\rm bond}(\ell) = k_q(\ell - R_b)^3(\ell - R_b - B_2)$. As in Refs. [28,29], we set $B_2 = -0.4668a$ and $k_q = 4431\varepsilon/a^4$; this sets the length of *unstretched* covalent bonds to $\ell_0 \simeq 0.96a$. Variable chain stiffness is modeled using the standard potential $U_{\rm ang}(\theta) = \kappa u_0[1 - \cos(\theta)]$, where θ is the angle between consecutive covalent-bond vectors and is zero for straight trimers.

All systems were equilibrated under standard melt conditions (monomer number density $\rho_{\rm melt} = 0.85/a^3$, temperature $T_{\rm melt} = 1.0u_0/k_B$ [32]) as described in Ref. [36]. Then they were slowly cooled to $T = 0$ (at zero pressure) as described in Ref. [35]. After cooling, systems were subjected to uniaxial-stress extension at a true strain rate $\dot{\epsilon} = 10^{-5}/\tau_{\rm LJ}$ or constant-volume simple shear at a strain rate $\dot{\gamma} = 10^{-5}/\tau_{\rm LJ}$, where $\tau_{\rm LJ} = \sqrt{ma^2/u_0}$ is the Lennard-Jones time unit [29]. Here we are focusing on the athermal ($T \to 0$) limit to isolate the dependence of G_R on chain stiffness from its dependence on temperature. In general, $G_R(\kappa, T) \simeq G_R(\kappa, 0)[1 - T/T_g(\kappa)]$, where T_g is the glass transition temperature [7,13].

Under standard melt conditions, these polymers' equilibrium Kuhn lengths are approximately [36]

$$\begin{aligned}\frac{\ell_K}{\ell_0} \approx{}& \frac{2\kappa + \exp(-2\kappa) - 1}{1 - \exp(-2\kappa)(2\kappa + 1)} \\ &+ 0.364(\tanh[0.241\kappa^2 - 1.73\kappa + 2.08] + 1), \end{aligned} \quad (2)$$

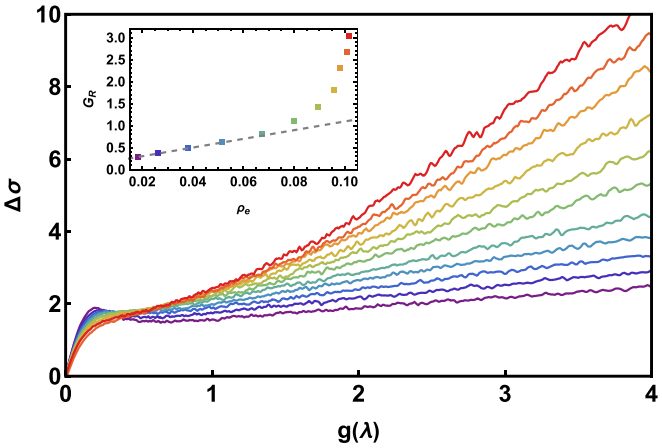

FIG. 1. Stress-strain curves for athermal uniaxial-stress extension of Kremer-Grest glasses with $0.5 \leqslant \kappa \leqslant 5.5$. Colors vary from purple to red with increasing κ. The inset shows the G_R values obtained by fitting these curves to Eq. (4) and a fit of results for $\kappa \leqslant 2.0$ to the expected linear scaling [7].

and their equilibrium entanglement lengths are [36]

$$N_e(\kappa) \simeq 80.5 - 70.4\tanh(\kappa/1.579). \quad (3)$$

All systems contained 4×10^5 monomers and had chain lengths $N \gtrsim 20N_e$, so finite-system-size and finite-N corrections to the results presented below should be minimal [28,35]. The simulated systems spanned nearly the entire range of positive κ ($0.5 \leqslant \kappa \leqslant 5.5$) for which melts remain isotropic under these conditions [33], and a range of N_e/C_∞ values ($1 \leqslant N_e/C_\infty \lesssim 28$) that is wider than the range spanned by real flexible and semiflexible polymer melts [22,37]. Following standard procedure [13,30], we assume that the glasses' ℓ_K and N_e values are inherited from their parent melts and are given by Eqs. (2) and (3). Thus their entanglement densities are $\rho_e(\kappa) = \rho_g(\kappa)/N_e(\kappa)$, where $\rho_g(\kappa)$ are the monomer number densities at $T = 0$. All quantities discussed below are expressed in dimensionless units.

III. RESULTS

Uniaxial stress-strain curves for all systems are shown in Fig. 1. Lower-κ systems have larger initial elastic moduli and larger yield stresses owing to their more-efficient segmental packing [35], but all systems have comparable stresses in the plastic-flow regime. As deformation continues, all systems exhibit a gradual crossover to standard "Gaussian" strain hardening described by [1]

$$\Delta\sigma(\lambda) = \sigma_{\rm flow} + G_R g(\lambda); \quad (4)$$

here $\lambda = \exp(\epsilon)$ is the stretch along the tensile direction and $g(\lambda) = \lambda^2 - 1/\lambda$ [38]. At even larger strains (not shown here), systems exhibit a crossover to nonlinear (Langevin [2,4]) strain hardening that becomes more dramatic with increasing κ. All of these stress-strain curves are qualitatively consistent with those reported in previous comprehensive simulations of glassy-polymeric strain hardening [13–15]; the only novel aspect is that here they span a much wider range of κ and ℓ_K/ℓ_0.

We estimate all systems' $G_R(\kappa, 0)$ by fitting their stress-strain curves to Eq. (4) over the range $2 \leqslant g(\lambda) \leqslant 4$. The inset shows how the resulting G_R values vary with $\rho_e(\kappa)$. As expected [7,13], we find that G_R is linearly proportional to ρ_e for flexible polymer glasses. More specifically, we find that $G_R \simeq c_0 + c_1\rho_e$ for systems with $0.5 \leqslant \kappa \leqslant 2.0$, and that while c_0 and c_1 are both sensitive to the range of $g(\lambda)$ used to estimate G_R, the overall result is robust. For larger κ, however, the expected $G_R \sim \rho_e$ scaling breaks down. G_R continues to increase steadily with increasing κ, whereas $d\rho_e/d\kappa$ *decreases* steadily as $N_e(\kappa)$ approaches its minimum possible value ($N_e^{\min} \simeq C_\infty$) for systems lacking long-range nematic order [20,21]. As a consequence, $dG_R/d\rho_e$ increases steadily and appears to diverge as κ approaches its isotropic-nematic transition value $\kappa_{\rm in}$ (which is slightly above 5.5 for the standard Kremer-Grest melt [33]). Notably, the range of κ for which the linear scaling fails (i.e., $2.5 \leqslant \kappa \leqslant 5.5$) corresponds to the range $1 \leqslant N_e/C_\infty \lesssim 4$, i.e., the range of N_e/C_∞ values corresponding to SCPs [21,22].

The observation that G_R is not always linearly proportional to ρ_e is an additional piece of evidence that entanglements only indirectly control strain hardening. One obvious candidate for the structural feature that *does*, in fact, directly control it is Kuhn segments [6–11]. Flory's definition of the characteristic ratio is

$$C_\infty = \left(\frac{1 + \langle\cos(\theta)\rangle}{1 - \langle\cos(\theta)\rangle}\right)\left(\frac{1 + \langle\cos(\psi)\rangle}{1 - \langle\cos(\psi)\rangle}\right), \tag{5}$$

where ψ is the dihedral angle formed by three consecutive covalent-bond vectors. $C_\infty = \ell_K/\ell_0$ in *undeformed* glasses, but it can increase dramatically over the course of applied deformation as $\langle\cos(\theta)\rangle$ and $\langle\cos(\psi)\rangle$ evolve. It has long been known that tensile plastic deformation in polymer glasses occurs largely through irreversible dihedral transitions that tend to increase $\langle\cos(\psi)\rangle$ [9], and Ref. [29] showed that the ratio $C_\infty(\lambda)/C_\infty(1)$ closely tracks $\Delta\sigma(\lambda)$ in the same systems considered here.

Predicting how polymer glasses' $\langle\cos(\theta)\rangle$ and $\langle\cos(\psi)\rangle$ evolve under applied deformation is very challenging, however, and therefore so is developing a Kuhn-segment-based theory of strain hardening using this approach. The phenomenological theory recently developed by Merlette *et al.* [39,40] employs a closely related approach, attributing strain hardening to the increasing free energy barriers for α relaxation that arise from the increasing local alignment of Kuhn segments. However, this theory does not explicitly address how G_R varies with ℓ_K/ℓ_0, and indeed it predicts that the length scale controlling these free energy barriers ($\xi =$ 3–5 nm) is considerably larger than ℓ_K. While it does predict that G_R scales approximately linearly with the "monomer" volume a^3, it treats a as an adjustable parameter rather than as a quantity that is precisely specified by polymer chemistry.

Another candidate for the controlling structure is statistical segments, which (unlike Kuhn segments) are effectively rigid and hence lack dynamic internal variables like θ and ψ. Statistical segments are the "atoms" of Chen and Schweizer's microscopic-physics-based polymer nonlinear Langevin equation (PNLE) theory of glassy polymer mechanics [41–43]. The PNLE predicts that strain hardening is a consequence of increasingly anistropic single-chain and intermolecular correlations that suppress long-wavelength density fluctuations [as encoded in the low-q limit of the static structure factor $S(q)$] and hence increase the instantaneous elastic shear modulus G. It predicts $G \sim k_BT/b^3$ for *fixed* $S(q)$ and $r_{\rm loc}/b$ (where $r_{\rm loc}$ is the "localization length"), but since both of these measures are strongly thermal- and deformation-history dependent, it does not predict a simple universal relationship between G_R and b.

Here we take an alternative approach that is much less rigorous than those employed in Refs. [39–43], but allows us to make such a prediction. Consider a semiflexible pearl-necklace-like polymer where the monomer diameter and covalent bond length are both ℓ_0 and the intermonomer binding energy is u_0. Since statistical segments are effectively rigid, it is reasonable to assume that the range of elastic intermonomer interactions is of order b, and therefore that the total elastic strain energy per monomer in a deformed glass composed of these polymers scales as $u_0(b/\ell_0)^3$. The associated energy density is $\mathcal{E} \sim (u_0/\ell_0^3)(b/\ell_0)^3$. Then, assuming that these glasses act like neo-Hookean solids and their strain energy density is $U \sim \mathcal{E}\tilde{g}(\bar{\lambda})$ leads to a normal stress difference $\Delta\sigma \sim \mathcal{E}g(\bar{\lambda})$ consistent with Gaussian strain hardening, with $G_R \propto (u_0/\ell_0^3)(b/\ell_0)^3 \equiv (u_0/\ell_0^3)(\ell_K/\ell_0)^{3/2}$.

Obviously glassy polymers are *not* elastic solids; the majority of the work done in deforming them beyond their yield points is dissipated as heat [44,45]. A simple interpretation of the prediction $G_R \propto b^3$ that is consistent with this experimental fact is that G_R is proportional to the number of noncovalent intermonomer "bonds" (e.g., van der Waals bonds) that must be "broken" for a Kuhn volume to plastically rearrange via irreversible changes in its constituent chains' $\{\theta\}$ and $\{\psi\}$. This interpretation is consistent with simulations that have shown that the rate of noncovalent bond rearrangments $R_{\rm P}$ scales with the dissipative component of $\Delta\sigma$ during strain hardening [14,15]. In particular, these studies found that $R_{\rm P}(\lambda) \simeq R_{\rm P}^{\rm flow} + \mathcal{R}_{\rm P}g(\lambda)$, and the variation of $\mathcal{R}_{\rm P}$ with chain stiffness tracks that of G_R. On the other hand, previous studies [15,35,46] suggest that the breakdown of $G_R \sim \rho_e$ scaling is *also* associated with energetic contributions to strain hardening that increase faster than ρ_e with increasing chain stiffness. Preliminary analyses indicate that this is indeed the case for our $\kappa \gtrsim 2.5$ systems, but owing to the complicating factors discussed in Sec. IV, further exploration of this possibility is deferred to future work.

While the above arguments specify how G_R should scale with b, they do not specify its magnitude. Inspired by Frenkel's classic yield criterion ($\tau_{\rm Y} = \mu/5$, where $\tau_{\rm Y}$ is the ideal strength of a material and μ is its shear modulus [47]) as well as more recent work showing that metallic glasses' $\tau_{\rm Y} \simeq \gamma_{\rm c}\mu$ (where $\gamma_{\rm c} \simeq 1/37.5$ is a critical shear strain [48]), we postulate that $G_0 = \mathcal{S}_{\rm c}(u_0/\ell_0^3)$ with $\gamma_{\rm c} < \mathcal{S}_{\rm c} \leqslant 1/5$. Here $\mathcal{S}_{\rm c}$ is the incremental elastic strain required to activate the above-mentioned cooperative Kuhn-segment-scale plastic rearragements, and b^3 is the volume of the associated shear transformation zones [49,50]. $\mathcal{S}_{\rm c}$ should be larger than $\gamma_{\rm c}$ because polymer glasses' yield strains are substantially larger than those of metallic glasses [9]. In this picture, Eq. (1) captures how the normal stress difference required to activate these rearrangements increases with large-scale chain orientation. This could offer a particularly simple explanation

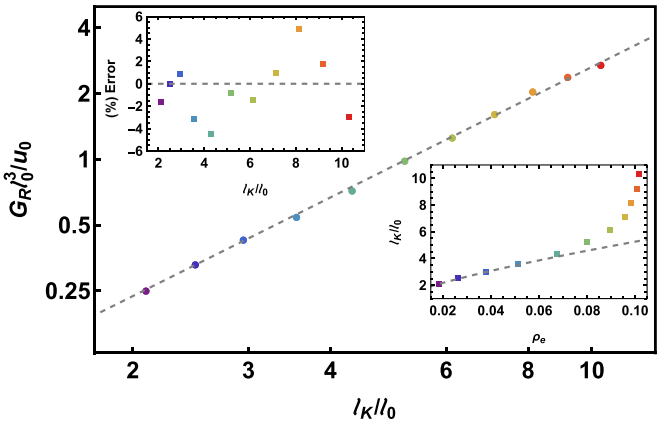

FIG. 2. Scaled strain-hardening moduli $G_R/(u_0/\ell_0^3)$ for athermal uniaxial-stress extension (colored symbols), and a fit of these data to $G_R = S_c(u_0/\ell_0)^3(\ell_K/\ell_0)^{3/2}$ with $S_c = (8.36 \pm 0.08) \times 10^{-2}$ (dashed line). The upper and lower insets respectively show the fractional errors associated with this fit and a plot of ℓ_K/ℓ_0 vs ρ_e.

for why G_R values can be $\sim 10^2$ times larger than $\rho_e k_B T$ even for T that are relatively near to T_g [7,8]. Specifically, $G_R \gg \rho_e k_B T$ in these systems because the free energy density that sets the magnitude of G_R is $\mathcal{S}_c(u_0/\ell_0^3)(b/\ell_0)^3$ rather than $\rho_e k_B T$.

We now demonstrate that the above assumptions allow us to formulate a theory that can quantitatively predict athermal G_R values for the Kremer-Grest model. Figure 2 plots the scaled moduli $G_R\ell_0^3/u_0$ obtained from our molecular dynamics simulations versus ℓ_K/ℓ_0. Remarkably, all data fall on the line $G_R\ell_0^3/u_0 = 0.0836(\ell_K/\ell_0)^{3/2}$ to within our estimated statistical and systematic errors. The fractional deviations between the fit and measured values of G_R are all less than 6%, which is comparable to the deviations from the predicted $\ell_K(\kappa)$ [Eq. (2)] reported in Ref. [36] and the dependence of the ratios of different G_R on the range of $g(\lambda)$ used to fit the stress-strain curves to Eq. (4). Moreover, the prefactor (0.0836) lies well within our estimated range for $\mathcal{S}_c$.

Are the theoretical arguments leading to Eq. (1) robust? Constant-volume simple shear provides a more stringent test because stresses are triaxial and include both tensile and compressive components. As a consequence, systems exhibit a greater tendency to deform inhomogeneously (via shear banding [9,30]). For our deformation protocol [29,35], the principal tensile and compressive stretches are respectively $\lambda_1 = (\sqrt{\gamma^2+4}+\gamma)/2$ and $\lambda_2 = (\sqrt{\gamma^2+4}-\gamma)/2$, with associated principal stresses

$$\sigma_{1,2} = (\sigma_{yy}+\sigma_{zz})/2 \pm \sqrt{(\sigma_{yy}-\sigma_{zz})^2/4 + \sigma_{yz}^2}. \qquad (6)$$

The normal stress difference is $\Delta\sigma \equiv \sigma_1 - \sigma_2$, and Gaussian strain hardening corresponds to

$$\Delta\sigma(\gamma) = \sigma_{\rm flow} + G_R g(\gamma), \qquad (7)$$

where $g(\gamma) = \lambda_1^2 - \lambda_2^2 \equiv \gamma\sqrt{4+\gamma^2}$. Stress-strain curves for all systems are shown in Fig. 3(a). $\kappa = 0.5$ systems shear band upon yielding as indicated by the long post-yield plateau in their $\Delta\sigma$, but all other systems exhibit a gradual crossover

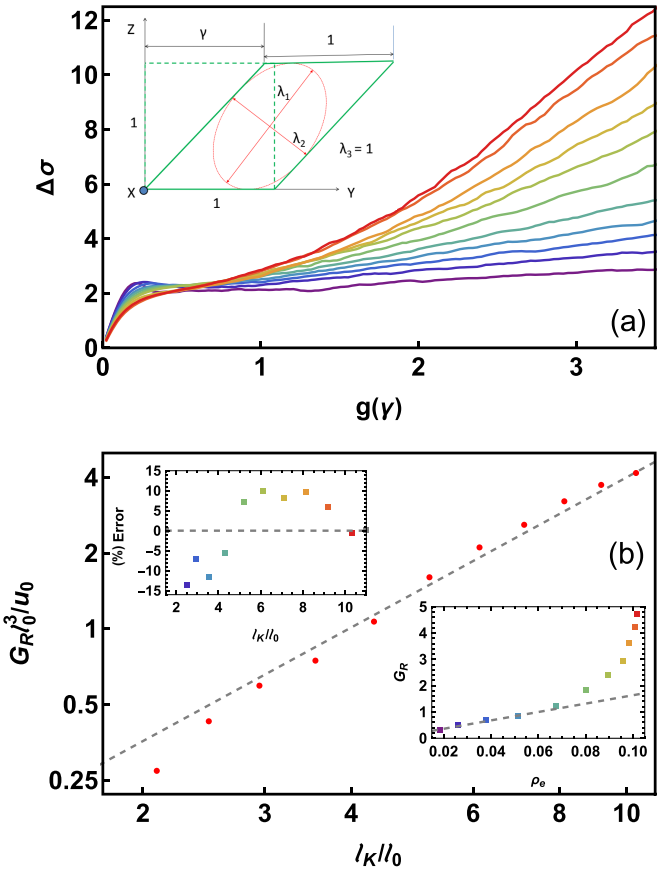

FIG. 3. Constant-volume simple-shear response for the systems analyzed in Figs. 1 and 2. Panel (a) shows the stress-strain curves; the inset schematically illustrates the principal stretch directions. Panel (b) shows the G_R values obtained by fitting these curves to Eq. (7) along with a fit to $G_R = G_0(\ell_K/\ell_0)^{3/2}$ scaling. The upper-left inset shows the fractional errors associated with this fit, while the lower-right inset shows a fit of the results for $\kappa \leqslant 2.0$ to the expected $G_R \sim \rho_e$ scaling [7].

to Gaussian hardening over the range $0.5 \lesssim g(\gamma) \lesssim 2$ that is similar to that shown in Fig. 1.

If our theoretical picture is correct, we would expect to find that $\Delta\sigma(\gamma) = \sigma_{\rm flow} + \mathcal{S}_c(u_0/\ell_0^3)(\ell_K/\ell_0)^{3/2}g(\gamma)$, where $\mathcal{S}_c$ can differ from the value obtained above (owing to the different strain geometry), but only by a factor of order one. Figure 3(b) shows the G_R obtained by fitting these stress-strain curves to Eq. (7) over the range $2 \leqslant g(\gamma) \leqslant 3.5$. Once again, the classic $G_R \sim \rho_e$ scaling holds for flexible polymers but breaks down for semiflexible polymers. For $\kappa > 0.5$, the hardening moduli instead are (once again) roughly linear in b^3.

Fitting these moduli to $G_R = S_c(u_0/\ell_0^3)(\ell_K/\ell_0)^{3/2}$ yields $S_c \simeq 0.127 \pm 0.004$, a value that is both within our estimated range for $\mathcal{S}_c$ and within an $\mathcal{O}(1)$ factor of the value obtained for uniaxial-stress tension. However, in contrast to the unaxial-stress case, the agreement is only *semi*quantitative. The rms fractional deviation between the fit and measured G_R for $\kappa > 0.5$ is 12.6%, which is five times larger than the corresponding deviation for uniaxial stress, and is too large to be explained by the above-mentioned statistical and systematic uncertainties in ℓ_K and G_R. Moreover, the deviations appear to

increase (decrease) systematically with κ for $\kappa \lesssim 3$ ($\kappa \gtrsim 4.5$). We expect that these trends arise from other factors that are not captured by our simple model, e.g., the greater tendency for heterogeneous deformation and earlier onset of Langevin hardening in simple shear [4]. Nevertheless, $G_R \sim (\ell_K/\ell_0)^{3/2}$ scaling clearly describes this dataset far better than $G_R \sim \rho_e$ scaling does.

IV. DISCUSSION AND CONCLUSIONS

The lower-right inset in Fig. 2 shows that ℓ_K/ℓ_0 (much like G_R) increases linearly with ρ_e for $\kappa \leqslant 2.0$ but faster than linearly for $\kappa \gtrsim 2.5$. This suggests that the failure of $G_R \sim \rho_e$ scaling can be physically interpreted as follows: G_R is actually scaling with another quantity (specifically, ℓ_K/ℓ_0) that itself scales linearly with ρ_e *for flexible systems*, and therefore the $G_R \sim \rho_e$ scaling observed for these systems indicates correlation rather than causation.

Van Melick *et al.*'s results for PS/PPO blends [7] are consistent with this interpretation because the PPO weight fraction $f_{\rm PPO}$ (which itself scales linearly with ρ_e) controls these systems' average segment-scale structure and interactions, and hence their effective $\langle (u_0/\ell_0)^3 b^3 \rangle$. Their demonstration that $G_R \propto (\rho_e + \rho_x)$ in pure PS with a wide range of cross-link densities ρ_x is harder to rationalize since these systems had nearly fixed b and u_0, but it could also be consistent with Eq. (1) if cross-links increase $\mathcal{S}_{\rm c}$ by suppressing Kuhn-segment-scale plastic rearrangements. Such increases would be consistent with their hypothesis that cross-links increase G_R by reducing segmental *mobility*.

This interpretation is also naturally consistent with the notion that entanglements play only an indirect role in controlling strain hardening, and specifically with the hypothesis that by forcing chains to deform affinely on chemical length scales $n > N_e$, they make polymer glasses neo-Hookean. While this idea was proposed long ago [5,6] and is assumed to be correct in modern theories of glassy-polymer mechanics [39–43], it had previously been difficult to demonstrate conclusively in the absence of evidence that $G_R \propto \rho_e$ scaling is nonuniversal. Violations of this scaling were previously reported only in simulations of binary mixtures of long ($N \gg N_e$) and short ($N \ll N_e$) chains, which found that G_R was linear (while ρ_e was quadratic) in the long chains' weight fraction f [51], and the conclusions of that study have been criticized on the grounds that such mixtures are brittle in experiments unless $1 - f \ll 1$ [52,53].

In conclusion, we have shown in this paper that $G_R \propto \rho_e$ scaling breaks down as N_e/C_∞ decreases into the regime corresponding to SCPs [22–27]. We have also taken a *first* step towards improving our ability to theoretically predict semiflexible polymer glasses' strain-hardening response by formulating a simple theory that can quantitatively predict the Kremer-Grest bead-spring model's athermal G_R values from its statistical- and Kuhn-segment-scale structure and interactions, over a range of N_e/C_∞ values ($1 \lesssim N_e/C_\infty \lesssim 28$) that is wider than the range spanned by real systems. This model, despite its simplicity, has been convincingly shown to capture many features of real polymer glasses' nonlinear mechanical response [11]. On the other hand, as detailed below, multiple assumptions we made while developing the theory presented above *greatly* oversimplify the structure and mechanics of real polymer glasses, and multiple challenges must be overcome before it can be fully validated at the microscopic level and/or for a wider range of model polymers and testing conditions.

First, while it predicts that $G_R = \mathcal{S}_{\rm c}(u_0/\ell_0^3)(b/\ell_0)^3$, here we have only studied how G_R varies with b in a model with fixed u_0 and ℓ_0. One seemingly obvious follow-up test would be to study the variation of G_R with u_0, but since u_0 is the only energy scale in athermal Kremer-Grest glasses, all stresses necessarily scale linearly with u_0 and therefore so will G_R. This observation raises a fundamental question: What will happen in polymer glasses with an additional athermal energy scale, e.g., the energy barrier for dihedral transitions? This question is not addressed by any published theoretical model and therefore remains open. Careful studies of strain hardening in atomistic or united-atom-model semiflexible polymers could provide answers, but fine-grained computational modeling of these polymers (many of which were synthesized only within the past few years [22,26]) began only recently [54,55], and it has not yet been applied to study their mechanical properties in the glassy state.

Second, comparing it directly to experiments will require both extrapolation of measured $G_R(T)$ values to the $T \to 0$ limit and accurate measurements of u_0, ℓ_0, and b. Such data is not yet readily available in the literature, but the above-mentioned extrapolation might be assisted by extending the theory to account for thermalization of the Kuhn-segment-scale plastic rearrangements and hence to predict how G_R depends on both T and strain rate [48]. Note, however, that the lack of $G_R(T)$ data for a wide range of polymer chemistries at $T \ll T_{\rm room}$ similarly impedes full validation of competing theories that already account for thermalization [39–43].

Third, it was only designed to treat *single-component* polymer glasses with well-defined values of u_0, ℓ_0, and b. A logical follow-up test would be to study blends of flexible and semiflexible bead-spring polymers to determine whether their G_R scale linearly with their $\langle (u_0/\ell_0)^3 (b/\ell_0)^3 \rangle$. Doing so would mirror the experiments on PS-PPO blends by van Melick *et al.* [7]. Unfortunately, methods for verifiably equilibrating such blends have not yet been developed for chain lengths $N \gg N_e$, and doing so may present multiple challenges, including their tendency to either macro- or microphase separate [56] at $T = T_{\rm melt}$ or during slow cooling into the glassy state (like that employed in our simulations).

Fourth, our implicit assumptions that elastic interactions have a sharp cutoff at a distance b, and that breaking of noncovalent bonds and plastic rearrangements of Kuhn segments are binary propositions, are, *at best*, oversimplifications. Stress correlations during plastic deformation of 3D amorphous materials tend to decay cubically with distance [i.e., $C_{\bar\sigma}(r) \equiv \langle \bar\sigma(\vec r_0)\bar\sigma(\vec r_0 + \vec r)\rangle - \langle \bar\sigma(\vec r_0)^2\rangle \sim (\Lambda/r)^3$, where brackets indicate averaging over all $\vec r_0$], and configurational measures of local plastic deformation such as neighbor rearrangements or locally nonaffine displacements decay similarly (see Refs. [57,58] for recent reviews). In polymeric glasses, the associated length scales (e.g., Λ) and the energy dissipated per plastic event can depend on deformation geometry and can increase as deformation proceeds, particularly for semiflexible polymers exhibiting Langevin hardening [15,35,46]. Since the theory of amorphous materials' plastic deformation remains

in a state of rapid development [59], there is not yet a consensus on how to handle such complicating factors.

Fifth, our assertion that G_R values scale with a power of the *statistical*-segment length remains questionable. Since $b \equiv \sqrt{\ell_0 \ell_K}$, $G_R \sim b^3$ scaling is formally equivalent to $G_R \sim \ell_K^{3/2}$ scaling. Moreover, polymers continuously rather than discretely stiffen as the examined length scale decreases, and neither b nor ℓ_K are uniquely fundamental length scales for real polymers in which the definition of a monomer can be somewhat arbitrary. Here we have chosen to focus on statistical segments largely because (i) they are the "atoms" of and are treated as rigid bodies in the highly successful PNLE theory [41–43], and (ii) we recently showed that assuming that Kuhn segments are composed of $\sqrt{C_\infty}$ rigid statistical segments allows one to predict that glassy polymers' craze extension ratio is $\lambda = (N_e/\sqrt{C_\infty})^{1/2}$ and hence that, contrary to expectations based on Kramer's classic prediction $\lambda = (N_e/C_\infty)^{1/2}$ [30], semiflexible polymers with $N_e = C_\infty$ can exhibit stable craze drawing [28,29].

Addressing any of the above issues would require extensive, careful follow-up studies that are beyond the scope of the present effort, which aimed to formulate a "cartoon-level" theory that is *useful* for understanding semiflexible polymer glasses' strain-hardening response and is consistent with the spirit of modern scaling theories for semiflexible polymer melts [19,20]. Addressing all of them (and in particular, the first, second, and fourth issues, which are not tied to any specific theoretical formulation) presents a challenge for the glassy-polymer-mechanics community.

ACKNOWLEDGMENTS

We thank Kang Chen, Kenneth Schweizer, Didier Long, David Simmons, Gary Grest, and Carsten Svaneborg for stimulating discussions, and two anonymous referees for numerous helpful comments. This material is based upon work supported by the National Science Foundation under Grant No. DMR-2026271.

DATA AVAILABILITY

All of the stress-strain data presented in Figs. 1 and 3 are available [60].

[1] A. S. Argon, Physical basis of distortional and dilational plastic flow in glassy polymers, J. Macromol. Sci. Part B: Phys. **8**, 573 (1973).

[2] R. N. Haward and G. Thackray, The use of a mathematical model to describe isothermal stress-strain curves in glassy thermoplastics, Proc. R. Soc. Lond. Ser. A **302**, 453 (1968).

[3] E. M. Arruda and M. C. Boyce, A three-dimensional constitutive model for the large stretch behavior of rubber elastic-materials, J. Mech. Phys. Solids **41**, 389 (1993).

[4] E. M. Arruda and M. C. Boyce, Evolution of plastic anisotropy in amorphous polymers during finite straining, Int. J. Plast. **9**, 697 (1993).

[5] R. N. Haward, The application of a simplified model for the stress-strain curves of polymers, Polymer **28**, 1485 (1987).

[6] R. N. Haward, Strain hardening of thermoplastics, Macromolecules **26**, 5860 (1993).

[7] H. G. H. van Melick, L. E. Govaert, and H. E. H. Meijer, On the origin of strain hardening in glassy polymers, Polymer **44**, 2493 (2003).

[8] E. J. Kramer, Open questions in the physics of deformation of polymer glasses, J. Polym. Sci. Part B: Polym. Phys. **43**, 3369 (2005).

[9] R. N. Haward and R. J. Young, *The Physics of Glassy Polymers* (Chapman & Hall, London, 1997).

[10] A. S. Argon, *The Physics of Deformation and Fracture of Polymers,* Cambridge Solid State Science (Cambridge University Press, Cambridge, UK, 2013).

[11] *Polymer Glasses,* edited by C. B. Roth (CRC, Boca Raton, FL, 2016).

[12] R. S. Hoy and M. O. Robbins, Effect of equilibration on primitive path analyses of entangled polymers, Phys. Rev. E **72**, 061802 (2005).

[13] R. S. Hoy and M. O. Robbins, Strain hardening of polymer glasses: Effect of entanglement density, temperature, and rate, J. Polym. Sci. Part B: Polym. Phys. **44**, 3487 (2006).

[14] R. S. Hoy and M. O. Robbins, Strain hardening in polymer glasses: Limitations of network models, Phys. Rev. Lett. **99**, 117801 (2007).

[15] R. S. Hoy and M. O. Robbins, Strain hardening of polymer glasses: Entanglements, energetics, and plasticity, Phys. Rev. E **77**, 031801 (2008).

[16] Y.-H. Lin, Number of entanglement strands per cubed tube diameter, a fundamental aspect of topological universality in polymer viscoelasticity, Macromolecules **20**, 3080 (1987).

[17] T. A. Kavassalis and J. Noolandi, New view of entanglements in dense polymer systems, Phys. Rev. Lett. **59**, 2674 (1987).

[18] L. J. Fetters, D. J. Lohse, D. Richter, T. A. Witten, and A. Zirkel, Connection between polymer molecular weight, density, chain dimensions, and melt viscoelastic properties, Macromolecules **27**, 4639 (1994).

[19] S. T. Milner, Unified entanglement scaling for flexible, semiflexible, and stiff polymer melts and solutions, Macromolecules **53**, 1314 (2020).

[20] R. S. Hoy and M. Kröger, Unified analytic expressions for the entanglement length, tube diameter, and plateau modulus of polymer melts, Phys. Rev. Lett. **124**, 147801 (2020).

[21] J. D. Dietz, M. Kröger, and R. S. Hoy, Validation and refinement of unified analytic model for flexible and semiflexible polymer melt entanglement, Macromolecules **55**, 3613 (2022).

[22] A. M. Fenton, R. Xie, M. P. Aplan, Y. Lee, M. G. Gill, R. Fair, F. Kempe, M. Sommer, C. R. Snyder, E. D. Gomez, and R. H. Colby, Predicting the plateau modulus from molecular parameters of conjugated polymers, ACS Cent. Sci. **8**, 268 (2022).

[23] J. Rivnay, R. M. Owens, and G. G. Malliaras, The rise of organic bioelectronics, Chem. Mater. **26**, 679 (2014).

[24] C. Liao, M. Zhang, M. Y. Yao, L. Li, and F. Yan, Flexible organic electronics in biology: Materials and devices, Adv. Mater. **27**, 7493 (2015).

[25] R. Xie, R. H. Colby, and E. D. Gomez, Connecting the mechanical and conductive properties of conjugated polymers, Adv. Electron. Mater. **4**, 1700356 (2018).

[26] R. Xie, A. R. Weisen, Y. Lee, M. A. Aplan, A. M. Fenton, A. E. Masucci, F. Kempe, M. Sommer, C. W. Pester, and E. D. Gomez, Glass transition temperature from the chemical structure of conjugated polymers, Nat. Commun. **11**, 893 (2020).

[27] S. H. K. Paleti, Y. Kim, J. Kimpel, M. Craighero, S. Haraguchi, and C. Müller, Impact of doping on the mechanical properties of conjugated polymers, Chem. Soc. Rev. **53**, 1702 (2024).

[28] J. D. Dietz, K. Nan, and R. S. Hoy, Unexpected ductility in semiflexible polymer glasses with entanglement length equal to their Kuhn length, Phys. Rev. Lett. **129**, 127801 (2022).

[29] K. Nan and R. S. Hoy, Craze extension ratio of semiflexible polymer glasses, Macromolecules. **56**, 8369 (2023).

[30] E. J. Kramer, Microscopic and molecular fundamentals of crazing, in *Crazing in Polymers*, edited by H. H. Kausch, Advances in Polymer Science (Springer, Berlin, Heidelberg,1983), Vol. 52–53, pp. 1–56.

[31] A. P. Thompson, H. M. Aktulga, R. Berger, D. S. Bolinteanu, W. M. Brown, P. S. Crozier, P. J. In t' Veld, A. Kohlmeyer, S. G. Moore, T. D. Nguyen, R. Shan, M. J. Stevens, J. Tranchida, C. Trott, and S. J. Plimpton, LAMMPS—a flexible simulation tool for particle-based materials modeling at the atomic, meso, and continuum scales, Comput. Phys. Commun. **271**, 108171 (2022).

[32] K. Kremer and G. S. Grest, Dynamics of entangled linear polymer melts: A molecular-dynamics simulation, J. Chem. Phys. **92**, 5057 (1990).

[33] R. Faller, A. Kolb, and F. Müller-Plathe, Local chain ordering in amorphous polymer melts: Influence of chain stiffness, Phys. Chem. Chem. Phys. **1**, 2071 (1999).

[34] M. J. Stevens, Interfacial fracture between highly cross-linked polymer networks and a solid surface: Effect of interfacial bond density, Macromolecules **34**, 2710 (2001).

[35] H. T. Nguyen and R. S. Hoy, Effect of the ratio ℓ_k/p on glassy-polymeric shear deformation mechanisms, Macromolecules **51**, 4370 (2018).

[36] J. D. Dietz and R. S. Hoy, Facile equilibration of well-entangled semiflexible bead–spring polymer melts, J. Chem. Phys. **156**, 014103 (2022).

[37] *Physical Properties of Polymers Handbook,* 2nd ed., edited by J. E. Mark (Springer, New York, 2007).

[38] This definition of $g(\lambda)$ ignores the very small increases in volume that occur at small strains, but correcting for these does not alter the main results presented below.

[39] T. C. Merlette, J. Hem, C. Crauste-Thibierge, S. Ciliberto, F. Clément, P. Sotta, and D. R. Long, Theory of plasticity and strain hardening of glassy polymers, Macromolecules **56**, 6510 (2023).

[40] T. C. Merlette, F. Clément, P. Sotta, and D. R. Long, Theory of Bauschinger and some other memory effects in glassy polymers, Macromolecules **58**, 3298 (2025).

[41] K. Chen and K. S. Schweizer, Microscopic constitutive equation theory for the nonlinear mechanical response of polymer glasses, Macromolecules **41**, 5908 (2008).

[42] K. Chen and K. S. Schweizer, Suppressed segmental relaxation as the origin of strain hardening in polymer glasses, Phys. Rev. Lett. **102**, 038301 (2009).

[43] K. Chen, E. J. Saltzman, and K. S. Schweizer, Molecular theories of segmental dynamics and mechanical response in deeply supercooled polymer melts and glasses, Annu. Rev. Condens. Matter Phys. **1**, 277 (2010).

[44] O. A. Hasan and M. C. Boyce, Energy storage during inelastic deformation of glassy polymers, Polymer **34**, 5085 (1993).

[45] D. J. A. Senden, S. Krop, J. A. W. van Dommelen, and L. E. Govaert, Rate- and temperature-dependent strain hardening of polycarbonate, J. Polym. Sci. Part B: Polym. Phys. **50**, 1680 (2012).

[46] R. S. Hoy, Why is understanding glassy polymer mechanics so difficult? J. Polym. Sci. Part B: Polym. Phys. **49**, 979 (2011).

[47] J. Frenkel, The theory of the elastic limit and the solidity of crystal bodies, Z. Phys. **37**, 572 (1926).

[48] W. L. Johnson and K. Samwer, A universal criterion for plastic yielding of metallic glasses with a $(T/T_g)^{2/3}$ temperature dependence, Phys. Rev. Lett. **95**, 195501 (2005).

[49] A. S. Argon, Plastic deformation in metallic glasses, Acta Metall. **27**, 47 (1979).

[50] M. L. Falk and J. S. Langer, Dynamics of viscoplastic deformation in amorphous solids, Phys. Rev. E **57**, 7192 (1998).

[51] R. S. Hoy and M. O. Robbins, Strain hardening in bidisperse polymer glasses: Separating the roles of chain orientation and interchain entanglement, J. Chem. Phys. **131**, 244901 (2009).

[52] J.-N. Liu, P.-P. Lin, S.-W. Cheng, W.-Y. Wang, J. W. Mays, and S.-Q. Wang, Polystyrene glasses under compression: Ductile and brittle responses, ACS Macro Lett. **4**, 1072 (2015).

[53] J-.N. Liu, Z.-C. Zhao, W.-Y. Wang, J. W. Mays, and S.-Q. Wang, Brittle-ductile transition in uniaxial compression of polymer glasses, J. Polym. Sci. Part B: Polym. Phys. **57**, 758 (2019).

[54] W. Zhang, J. H. Bombile, A. R. Weisen, R. Xie, R. H. Colby, M. J. Janik, S. T. Milner, and E. D. Gomez, Thermal fluctuations lead to cumulative disorder and enhance charge transport in conjugated polymers, Macromol. Rapid Commun. **40**, 1900134 (2019).

[55] A. E. Cohen, N. E. Jackson, and J. J. de Pablo, Anisotropic coarse-grained model for conjugated polymers: Investigations into solution morphologies, Macromolecules **54**, 3780 (2021).

[56] W. Peng, R. Ranganathan, P. Keblinski, and R. Ozisik, Viscoelastic and dynamic properties of well-mixed and phase-separated binary polymer blends: A molecular dynamics simulation study, Macromolecules **50**, 6293 (2017).

[57] A. Nicolas, E. E. Ferrero, K. Martens, and J.-L. Barrat, Deformation and flow of amorphous solids: Insights from elastoplastic models, Rev. Mod. Phys. **90**, 045006 (2018).

[58] D. Richard *et al.*, Predicting plasticity in disordered solids from structural indicators, Phys. Rev. Mater. **4**, 113609 (2020).

[59] L. Berthier, G. Biroli, L. Manning, and F. Zamponi, Yielding and plasticity in amorphous solids, Nat. Rev. Phys. **7**, 313 (2025).

[60] R. S. Hoy, The supporting data for Glassy polymers' strain-hardening moduli scale with their statistical-segment volumes, http://labs.cas.usf.edu/softmattertheory/PRLsubmissiondata-112025.tar.gz.